# Flow behaviour of pickering hexadecane emulsion stabilized with CNC and AOT for sustainable refrigeration

Pascal Clain, Somia Haouache, Isabelle Capron, Anthony Delahaye, Laurence Fournaison

Results in Engineering 27 (2025) 106494

Contents lists available at ScienceDirect

Results in Engineering

journal homepage: www.sciencedirect.com/journal/results-in-engineering

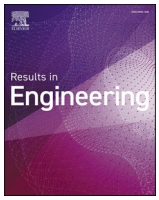

Research paper

# Flow behaviour of pickering hexadecane emulsion stabilized with CNC and AOT for sustainable refrigeration

Pascal Clain [a,b,*], Somia Haouache [b,c], Isabelle Capron [c], Anthony Delahaye [b], Laurence Fournaison [b]

[a] De Vinci Higher Education, De Vinci Research Center, Paris, France
[b] Université Paris-Saclay, INRAE, FRISE, 92761 Antony, France
[c] INRAE, UR BIA, 44316 Nantes, France

ARTICLE INFO

*Keywords:*
Rheology
Phase change material slurries
Pickering emulsion
Hexadecane
Cellulose nanocrystals
AOT

ABSTRACT

The rheological behaviour under flow conditions of hexadecane-in-water emulsions stabilized by cellulosic nanoparticles was studied with a capillary viscometer. The study investigated several volume fractions of hexadecane between 0 and 15 vol%. and the temperature was varied in situ to investigate the liquid and solid states of hexadecane droplets (below and above 18 °C respectively). Various concentrations of 0 to 1 vol% of anionic bis (2-ethylhexyl) sulfosuccinate sodium (AOT) were used as anti-agglomerant agent and to ensure the continuous flow. Based on the capillary viscometer method associated with Rabinowitsch and Mooney's equation, the apparent viscosity of these emulsions (hexadecane in liquid state), dispersions (hexadecane in solid state) was determined by measuring the pressure drops of the flowing fluid as a function of the flow rate. We observed that the viscosity of those systems increased with the volume fraction of hexadecane, both in liquid and solid state. We also observed that the viscosity can be decreased by cycling the emulsions in the loop. This decrease of viscosity was accompanied by a decrease of the mean droplets size measured by granulometry analysis. We showed in this work the important role of AOT to avoid emulsion agglomeration during the cooling in the loop.

## 1. Introduction

Refrigeration is a basic need for the population in many domains, such as food preservation, air conditioning, the chemistry industry, etc. Yet, refrigeration has an important impact on the environment and the effect of global warming. According to the International Institute of Refrigeration estimations ([1,2]), the refrigeration sector-related emissions account for 8% of global GHG emissions. Among these emissions, 63% is caused by the energy consumption of the refrigeration units and 37% is caused by refrigerant leakage. Due to the recent implementation of the Kigali Amendment to the Montreal Protocol, many refrigerants such as CFC (Chlorofluorocarbones), HCFC (Hydrochlorofluorocarbones) and HFC (Hydrofluorocarbones) are banned or their phasing down are in progress. The use of low GWP (Global Warming Power) refrigerant, such as (HFC or HFO (Hydrofluoroolefine)) or natural refrigerants (Ammonia, CO2, and hydrocarbon…) are now highly recommended. At the same time, the refrigeration sector - including air conditioning - consumes about 20% of the overall electricity used worldwide. Therefore, developing an energy-efficient refrigerating system implementing less refrigerant is essential. Secondary refrigeration loops using phase change material slurries is one technical solution that fulfils this ambition. Secondary refrigeration systems are usually less efficient than a direct system, but the implementation of slurries (two-phase solid-liquid fluids) can balance this drawback. Indeed, a slurry consists of a carrier fluid containing small particles of phase change material (PCM) as ice or paraffin. PCMs provide a large amount of energy when melting (when heat is absorbed) due to their latent heat of melting. Paraffins are of major interest in refrigeration systems thanks to their high latent heat [3–6] and adapted melting temperature for the application.

Emulsions are suitable for a wide variety of applications such as the petroleum industry, or the food, pharmaceutical and cosmetic industries [7–10]. It is also the best way to implement paraffin slurry in secondary refrigeration loops. In an emulsion, the PCM is encapsulated in tiny droplets, allowing the PCM to undergo phase transitions from liquid to solid or vice versa while the continuous phase remains in a liquid state,

* Corresponding author.
*E-mail address:* pascal.clain@devinci.fr (P. Clain).

https://doi.org/10.1016/j.rineng.2025.106494
Received 7 May 2025; Received in revised form 14 July 2025; Accepted 27 July 2025
Available online 28 July 2025

thereby ensuring smooth fluid flow within the refrigeration circuits.

The emulsions are stabilized by the presence of molecules at the oil-water interface. Usually, these are surfactants, also called emulsifiers. There are two other categories of interface stabilizers, polymers that can be entangled on the surface of the droplets and solid particles that will be irreversibly adsorbed at the oil-water interface, thus forming the so-called Pickering emulsions [11,12].

There has been a growing interest in the use of Pickering emulsions stabilized by solid nanoparticles [13,14]. These emulsions, known for their stability under challenging reservoir conditions, are being increasingly applied in the oil industry. Solid nanoparticles adsorb onto the oil-water interface, provided they possess the right degree of hydrophobicity. Once adsorbed, these particles become irreversibly anchored at the interface, forming a mechanical barrier that enhances the stability of the emulsion. Furthermore, the presence of colloidal particles at the oil-water interface significantly influences the rheological properties of the Pickering emulsion.

In the latter case, bio-based particles with a low environmental impact are therefore actively studied, such as nanocellulose. Since Oza and Frank [15] demonstrated that microcrystalline cellulose was able to form a network around oil droplets, many stabilized emulsions by nanocelluloses have been reported with cellulose nanofibrils [16,17], cellulose nanocrystals [18,19], and bacterial nanocellulose [20]. The flowability of a paraffin emulsion is a crucial parameter to the technical viability of the secondary refrigeration process based on this material. The rheological properties of emulsion-based materials play a major role in determining their suitability for particular applications [21,22]. In some applications, the rheological properties must remain constant throughout the emulsion use, while in others these rheological properties should change in response to a specific change in the environment, such as temperature, pH, stirring or dilution.

The rheology of an emulsion depends on several parameters: the formulation process, the rheology of the continuous phase, the nature and the volume fraction of the dispersed phase, the nature of stabilizer, the nature of the droplets (particle size distribution, deformability) and particle-particle interaction in the emulsion [23]. Generally, the viscosity of emulsions increases with the volume fraction of the dispersed phase [24–27]. This is not the case for the droplet size, which can influence differently the viscosity of the emulsions for the different systems. Schramm [28] and Pal [29] indicated that emulsion viscosity increases with increasing homogeneity, that is when the particle size distribution is narrow rather than wide. Abramov et al. [30] have shown that the viscosity of solid-state paraffin emulsions increases with increasing droplet sizes. Das et al. [31] and Rajagopal [32] have shown that it is difficult to distinguish between the effects of particle deformation and the effects of particle size distribution width on the rheological behaviour of emulsions. In addition to stability issues, paraffin emulsions are also subject to flow assurance problems. Sedimentation, agglomeration or plugging phenomena are very often observed in flow experiments. Anti-agglomerant additives such as Dioctyl Sodium Sulfosuccinate (AOT) [33] and Sodium Dodecyl Sulfate (SDS) [34,35] are commonly used to prevent these risks. AOT (Aerosol OT), the sodium salt of bis(2-ethylhexyl) sulfosuccinate, is a widely used anionic surfactant known for its remarkable ability to form emulsions without requiring additional cosurfactants. This surfactant can form reverse micelles in non-polar media, such as alkanes, which can encapsulate substantial amounts of water and form microemulsions, either as discrete droplets or bi-continuous networks. These properties make AOT highly versatile for various formulations, especially those where simplicity and reproducibility are critical [36,37]. Higuchi et al. [38] studied the aggregation in hexadecane-in-water emulsions containing AOT at varying concentrations. It was found that at low AOT concentrations ($\lesssim 0.1$ %) the emulsions were completely disaggregated. As the AOT concentration increased beyond this value, aggregation set in and progressively increased over the entire range of AOT concentration studied (up to 1.5 %). In this system, aggregation was found to be completely reversible, the equilibrium being reached in all cases in a few days. Several studies have investigated the thermophysical and rheological properties of hexadecane emulsions. Günther et al. [39] conducted experimental research on the supercooling behaviour of hexadecane emulsions. Zhang et al. [40] prepared n-hexadecane-based emulsions and explored their phase transition characteristics, rheological properties, and overall stability. In a related study, Morimoto et al. [41–43] formulated emulsions using both n-hexadecane and n-octadecane, and experimentally assessed their droplet size distributions, viscosities, flow behaviours, and latent heat storage capacities. Kawanami et al. [44] measured the viscosity, thermal conductivity, phase change behaviour, and long-term stability of emulsions composed of n-tetradecane, n-hexadecane, and n-octadecane, and further analyzed their heat transfer performance under relevant operational conditions. Chen et al. [45] studied the thermophysical and transport properties of n-hexadecane, and n-octadecane nano-emulsions in water. Zhang et al. [46] prepared n-hexadecane emulsions stabilized by SiO2 nano-particles. They analyzed the emulsion properties including emulsifier combinations and process conditions, interfacial film properties, droplet size distribution, and rheology characteristics. Giordano and Gschwander [47] evaluated the storage density, phase transition behaviour, supercooling, and dynamic viscosity of oil in water nano-emulsion of hexadecane at various concentrations. Shayanmehr and Eslami [48] studied the stability of hexadecane emulsions with various surfactants including AOT by carrying out several freeze-thaw cycles in a rotating viscometer.

The majority of works studying the effects of different parameters on the rheological behaviour of hexadecane emulsions have been carried out using rotational rheometers or controlled-strain rheometers by measuring the steady shear viscosity and/or dynamic viscoelasticity [47,49–54]. In this work, we present the first study on the rheological properties in flow loop using a capillary viscometer of hexadecane-in-water Pickering emulsions stabilized by cellulose nanocrystals (CNCs). Capillary viscometer enables to mimic realistic flow conditions encountered in secondary refrigeration systems, where such emulsions circulate under pressure in pipelines and experience shear stress due to pumping. The capillary viscometer enables the determination of flow-dependent rheological parameters under dynamic, flow-relevant shear rates that are more representative of industrial application conditions than those simulated in standard rheometers. A set of paraffin-based oil-in-water (O/W) emulsions with different PCM concentrations is prepared. The hexadecane content is varied between 0 to 15 vol % within distillated water. Hexadecane was stabilized by cellulose nanocrystals and a surfactant has been used to prevent particles agglomeration in solid state within the loop.

## 2. Materials and methods

### 2.1. Materials

The cellulose nanocrystals obtained by sulfuric acid hydrolysis of bleached Kraft pulp were purchased by CelluForce (Alberta Innovates Technology Futures (AITF) Montreal, Canada). Hexadecane (HD) (purity $\geq$ 99%, melting point at 18 °C) and Dioctyl Sodium Sulfosuccinate; AOT ($C_{20}H_{37}NaO_7S$, purity $\geq$ 99 %) [33,55] were acquired from Sigma Aldrich and used without further purification. The chemical structures are presented in Fig. 1. AOT is a white waxy solid that dissolves easily in alcohols and hydrocarbons. It has a molecular weight of 444.5 g/mol, a linear molecular length of 11 Å, and a polar headgroup area of approximately 55 Å$^2$. Structurally, the AOT molecule contains three chiral centers—at carbon atoms C1 (adjacent to the head group), C4, and C4'—yielding a total of eight possible optical isomers. Water was purified with the Milli-Q reagent system (18.2 MΩ cm Millipore Milli-Q purification system).

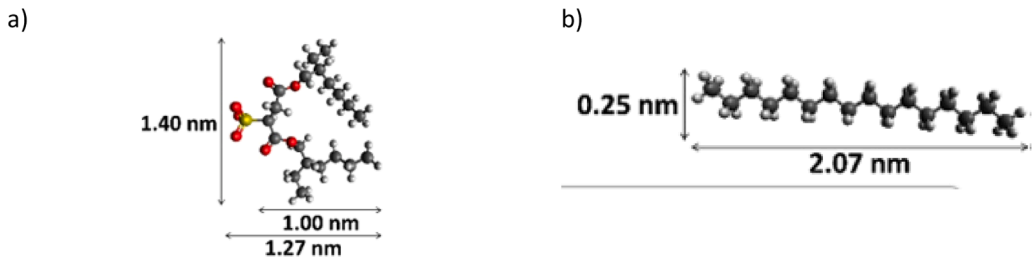


**Fig. 1.** Dimensions of AOT and hexadecane molecules calculated using Avogadro software [56].

### 2.2. Emulsion preparation and characterization

The hexadecane-in-water (H/W) Pickering emulsion was prepared at room temperature by mixing an aqueous dispersion of cellulose nanocrystals (CNCs) at 10.3 g/L in the presence of 50 mM NaCl (continuous phase) with hexadecane (dispersed phase) at a 30 vol % of hexadecane. Cellulose nanocrystals (CNCs) are nanorods 160 nm long and 10 nm thick that are known to irreversibly adsorb at the oil-water interface [20]. Their interfacial properties have been extensively studied, showing that they align along the surface as a monolayer [18]. CNCs are stable in aqueous suspension because of sulfate half ester groups on their surface that impart electrostatic repulsions. However, once adsorbed at the interface they might undergo electrostatic repulsions, therefore NaCl at low concentration (50 mM) was added in order to favor high density coverage on the surface of the droplets [19]. A volume of 500 mL of 30 vol % emulsion was mixed using a high-shear mixer, L5M-A Silverson mixer (Silverson Machines, Germany) at 5000 rpm for 8 min to obtain mean diameter of 15 μm as showed in Fig. 2. the concentration of CNCs was calculated to reach 24 mg of CNCs per mL of hexadecane. As shown in Fig. 2, no coalescence or Ostwald ripening process was observed since no significant change in droplet size was observed after two months of storage at room temperature.. This emulsion was then diluted with fresh water at 20 vol %, 15 vol %, 10 vol %, 5 vol % and 1 vol % of hexadecane with an absolute error of 0,94 vol % as described in Table 1. Since it was observed that the volume of water did not impact the droplets dimensions and creaming emulsion volume. Following dilution, AOT at different concentrations between 0 and 1 wt % was added to the emulsions. To ensure complete homogenization, the samples were stirred overnight using a magnetic stirrer. AOT ions tend to be miscible with apolar solvents but has limited miscibility with water [56].

### 2.3. Droplet diameters measurement

The average droplet surface mean diameter (also referred as D [3,2] or the Sauter mean diameter) was measured by laser light scattering using a Horiba LA-960 particle size distribution analyzer (Kyoto, Japan). An analysis model was used with a refractive index of 1.43 and 1.33 for HD and water, respectively. The calibration for water as a reference was taken before each measurement. All emulsions were measured at a range of transmittance between 80 and 90%. The measurements were systematically carried out in duplicate.

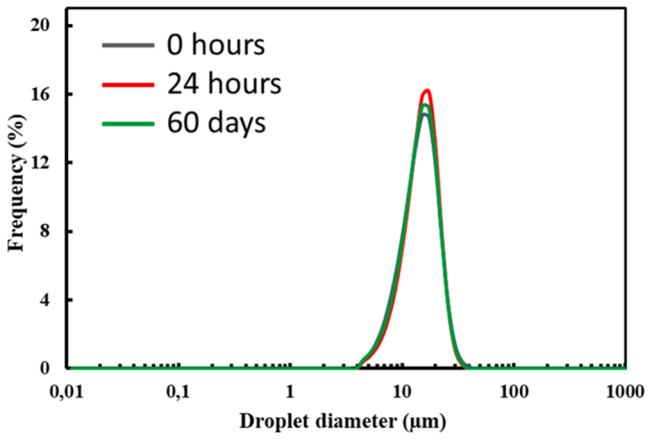


**Fig. 2.** Distribution of the droplet diameter of the emulsions showing long tearm stability.

**Table 1**
Hexadecane emulsion dilution preparation.

| HD emulsion concentration | Volume of emulsion at 30 vol % (mL) | Volume of pure water (mL) |
|---|---|---|
| 20 vol % | 333.3 | 166.6 |
| 15 vol % | 250 | 250 |
| 10 vol % | 166.6 | 333.3 |
| 5 vol % | 83.3 | 416.6 |
| 1 vol % | 16.6 | 483.3 |

### 2.4. Thermal analysis

The impact of the AOT concentration on the thermodynamics properties of the paraffin phase during phase transition was investigated during freezing and heating cycles. A Differential Scanning Calorimetry apparatus Q100 DSC (TA Instruments, USA) was used to carry out these calorimetry characterizations. The samples underwent the following thermal protocol: they were first cooled from 20 °C to 2 °C at a cooling rate of 2 °C per minute, followed by an isothermal hold at 2 °C for 2 min. Subsequently, the samples were heated from 2 °C to 35 °C at a rate of 3 °C per minute for a complete melting of hexadecane. Each DSC measurement was performed using sample masses ranging from 10 to 16 mg.

### 2.5. Rheological analysis

The rheological behaviour of H/W dispersions in liquid and solid state was studied with a capillary viscometer in a circulation loop. The experimental loop as illustrated in Fig. 3 is composed of 316 L stainless

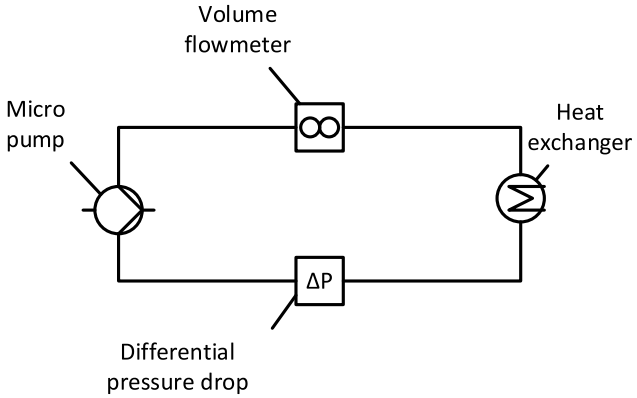


**Fig. 3.** Illustration of the experimental loop used for rheological experiments.

pipes with an internal diameter of 7.74 mm and an external diameter of 9.52 mm. The inner volume of the loop was determined at 0.480 L. It is equipped with a 220-type Axflow Micro Pump (adjustable speed, differential pressure of 0.4 MPa, static pressure of 10 MPa, flow rate pump max of 200 L/$h$ ± 0.04 %). The pump is controlled by a Leroy Somer speed variator. The flow rate is measured by an electromagnetic flowmeter ABB-type DS21 (0–1800 L/$h$ ± 0.5 %). The loop is equipped with 4 T-type thermocouples (±0.3 K) located in the solution at various positions. A differential pressure drop sensor is positioned after the pump and measures the pressure drop between two points spaced apart on a 50 cm straight section of the loop. All the sensors are connected to an acquisition system composed of an Agilent interface and a computer. The experimental device is placed in a temperature-controlled room (3.39 × 3.48 × 2.51 m). All the rheology results presented in this article have been subjected to a rigorous analysis of the propagation of uncertainties, in accordance with the methodology defined by the ISO/IEC Guide 98–3:2008 "Guide to the Expression of Uncertainty in Measurement" (GUM method) provided by the International Joint Committee for Guides in Metrology (JCGM), thus guaranteeing the traceability and reliability of the viscosities reported. The absolute uncertainty measurements for the data are given in Appendices A, B, C and D.

The experimental rheological protocol for the H/W emulsion characterization in atmospheric pressure at a given temperature consists first in loading the loop with the H/W emulsion at given volume fraction and then applying an initial flow rate. The rheological study was carried out after flow rate and temperature stabilization (25 °C for the liquid state of HD and 10 °C for the solid state) by varying the flow rate and measuring the corresponding pressure drops of the flowing fluid, as shown in Fig. 4.

As in previous works [57,58], the capillary viscometer method associated with Rabinowitsch and Mooney's equation [59] was used to characterize the rheological behaviour of H/W emulsions in order to determine the apparent viscosity ($\mu_{app}$) as a function of hexadecane fraction in the liquid and solid state. Several assumptions must be considered to apply the method: the H/W emulsion must be considered as pseudo-homogeneous and incompressible fluids, circulating in a laminar regime in the cylindrical pipe without wall slip. From a force balance on a section of fluid, relating pressure drop and stress, flow rate as a function of shear stress and shear rate can thus be represented by the following equation:

$$\frac{Q}{\pi R^3} = \frac{1}{4}\left(\frac{8U}{D}\right) = \frac{1}{\tau_w^3}\int_0^{\tau_w} \tau^2 \dot{\gamma} d\tau \tag{1}$$

Where $\tau_w$ is the shear stress at the wall in Pa, related to regular pressure drop ΔP in Pa due to a pipe of length L in m and diameter D in m:

$$\tau_w = \frac{D\,\Delta P}{4L} \tag{2}$$

After derivation of Eq. (1) with respect to $\tau_w$, the Rabinowitsch-Mooney equation [59], providing an expression of the shear rate at the wall, is obtained:

$$\dot{\gamma}_w = \frac{8U}{D}\frac{(3n+1)}{4n} \tag{3}$$

Where $n$ is the behaviour index which measures material deviation from Newtonian behavior and is defined as Eq. (4) and related to the flow velocity U in m/s:

$$n = \frac{d\ln\tau_w}{d\ln\frac{8U}{D}} \tag{4}$$

Thus, measurements of pressure drop ΔP and flow velocity U allow the determination of shear stress at the wall, behaviour index and shear rate at the wall, which can be modelled by the Herschel-Bulkley's Eq. (5) to express the rheological behaviour of the fluid:

$$\tau_w = \tau_0 + k\dot{\gamma}_w^n \tag{5}$$

Finally, the apparent viscosity $\mu_{app}$ of the emulsion is defined as a

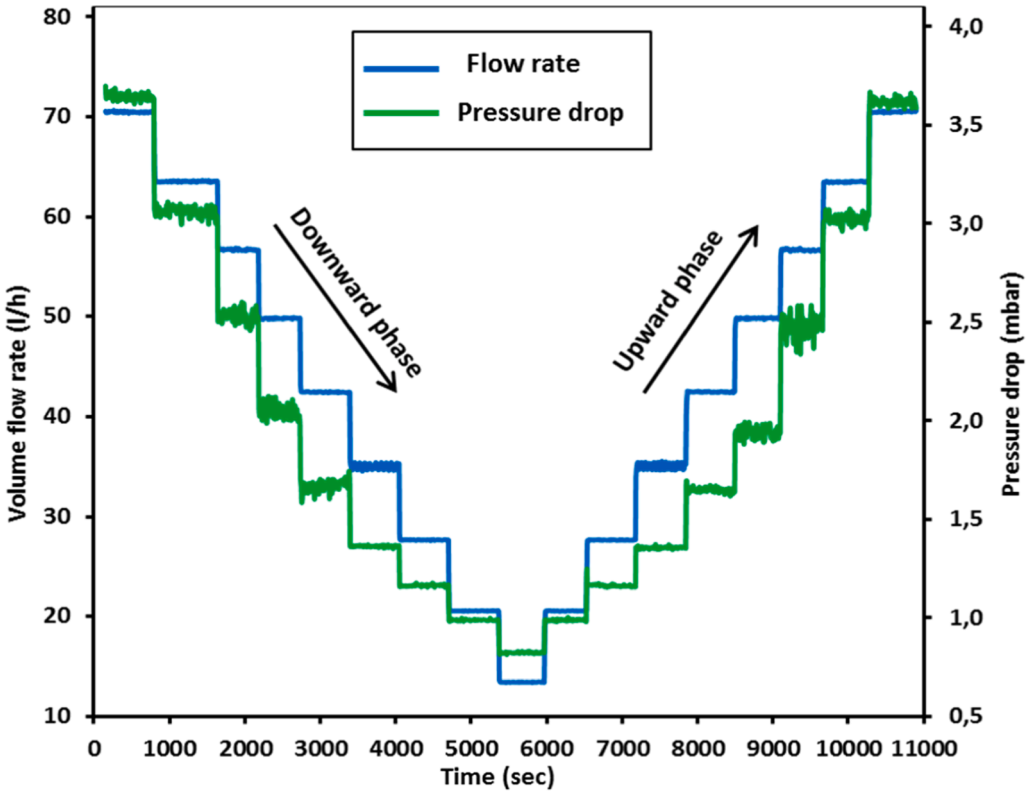


**Fig. 4.** Evolution of pressure drop at various flow rates.

ratio between the shear stress and the shear rate at the wall [60].

$$\mu_{app} = \frac{\tau_w}{\dot{\gamma}_w} \tag{6}$$

## 3. Results and discussion

### 3.1. Rheological behaviour of liquid and solid hexadecane emulsion in the loop

#### 3.1.1. Flow behaviour of liquid HD emulsion

Initially, the pressure drop and flow rate were measured over time in the liquid state of HD (at 25 °C) for emulsion concentrations ranging from 0 to 15 vol %. The behaviour index $n$ for each HD concentration was determined by analyzing the experimental data pair (ΔP, U), and it was calculated from the slope derived from Eq. (4). The evolution of the behaviour index $n$ as a function of the HD concentration is shown in Fig. 5a. It is noteworthy that the behaviour index $n$ decreases sharply as the HD concentration increases. At low concentrations between 0 and 3 %, the behaviour index $n$ experiences a steep decline, dropping from around 1 to roughly 0.5. This indicates that, at lower concentrations, the emulsion quickly shifts from behaving like a Newtonian fluid to exhibiting pseudoplastic characteristics. Following this initial drop, the curve stabilizes, with the behaviour index remaining around 0.5 for hexadecane concentrations ranging from 1 to 15 vol %.

The behaviour index $n$ can be represented by an asymptotic exponential relationship (Fig. 5a) as a function of the HD concentration (ranging from 0 to 15 vol %), as shown in Eq. (7):

$$n = 0.483 + 0.564 * 0.109^{\varnothing_{HD}} \tag{7}$$

The subsequent step involved simultaneously determining the other parameters of the general Herschel-Bulkley model, as described by Eq. (5), specifically the consistency index $k$ and the yield stress $\tau_0$. For each run, the consistency index $k$ is determined by a linear regression of $\tau_w$ as a function of $\dot{\gamma}_w^n$ where $k$ is the slope and the yield stress is the ordinate at origin. Results showed that the yield stress can be neglected. Fig. 5b illustrates the evolution of the consistency index $k$ as a function of the HD concentration ranging from 0 to 15 vol %. The consistency index $k$ increases linearly with the HD concentration. This linear increase in with HD concentration aligns with the typical behaviour of emulsions, where a higher volume fraction of the dispersed phase tends to increase the flow resistance [61,62].

The rheological model (Fig. 6) can be expressed by integrating the correlations of $n$ and $k$ into the Ostwald-de Waele model for HD concentration between 0 and 15 vol %:

$$\mu_{app} = k\dot{\gamma}_w^{n-1} = (0.004 * \varnothing_{HD} + 0.016) * \dot{\gamma}_w^{(0.483+0.564*0.109^{\varnothing_{HD}})-1} \tag{8}$$

The empirical method closely follows the trends of the experimental data across all concentration. For each HD concentration, the apparent viscosity decreases as the shear rate increases, exhibiting the characteristic behaviour of shear-thinning fluids, where viscosity decrease under greater shear stress. At higher HD concentrations, the apparent viscosity remains significantly higher at low shear rates, indicating increased viscosity of the emulsion at these concentrations. However, slight deviations are noted, particularly at low shear rates for concentrations of 5 vol % and 10 %. These variations maybe attributed to a lack of precision in the consistency index estimation for these experiments. Giordano and Gschwander [47] realized a rheological characterization of nanoemulsions of HD in water on a dynamic strain-controlled rheometer (median particle size of 0.5 μm) at various concentrations 10 to 40 wt % and found that the viscosity increases exponentially with the hexadecane content, particularly beyond 30–35 wt %, where the emulsions begin to show signs of instability and pronounced shear resistance and confirm the behaviour observed in our experiments. It also noticeable that despite having similar or even higher dispersed phase concentrations, their emulsions exhibit lower apparent viscosities—particularly evident at 10 vol %. This discrepancy can be attributed to the significant difference in droplet size distribution between the two studies. Their emulsions have a particle size distribution roughly ten times smaller than those used in the present work.

#### 3.1.2. Flow behaviour of solid H/W dispersion

In a second step, the loop temperature was decreased to around 7 °C to obtain a complete H/W crystallization, then, the pressure drop and flow rate were measured over time for dispersion concentrations ranging from 0 to 15 vol %. In our experiments, it was assumed that the solid conversion of H/W dispersion was fully completed, the phase change temperature of HD is 18 °C.. However, when the temperature reached 18 °C, both pressure drop and flow rate began to increase and their values failed to stabilize with time as illustrated in Fig. 7. This behaviour suggests H/W solid particles agglomeration within the loop causing the flow rate drop to zero, indicating a blockage in the loop.

To overcome clogging and agglomeration issues, we decided to add a well-known anti-agglomerant additive, AOT, to the hexadecane emulsion. In the following, we present the results of the impact of AOT on both emulsion stability and flow properties.

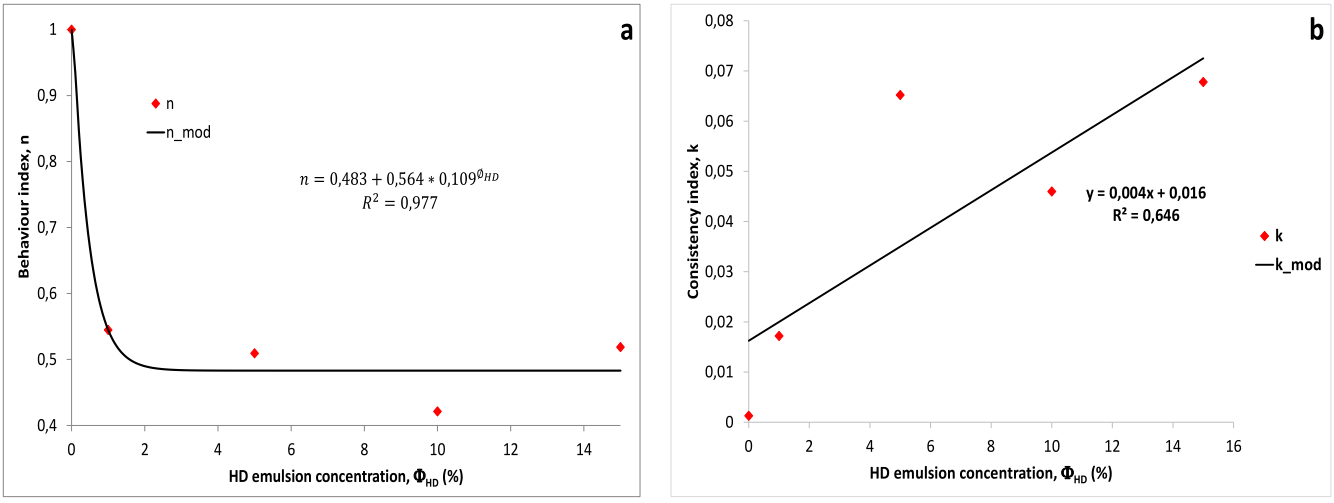


**Fig. 5.** Evolution of a) the behaviour index n and b) the consistency index k as a function of HD concentration ΦHD.

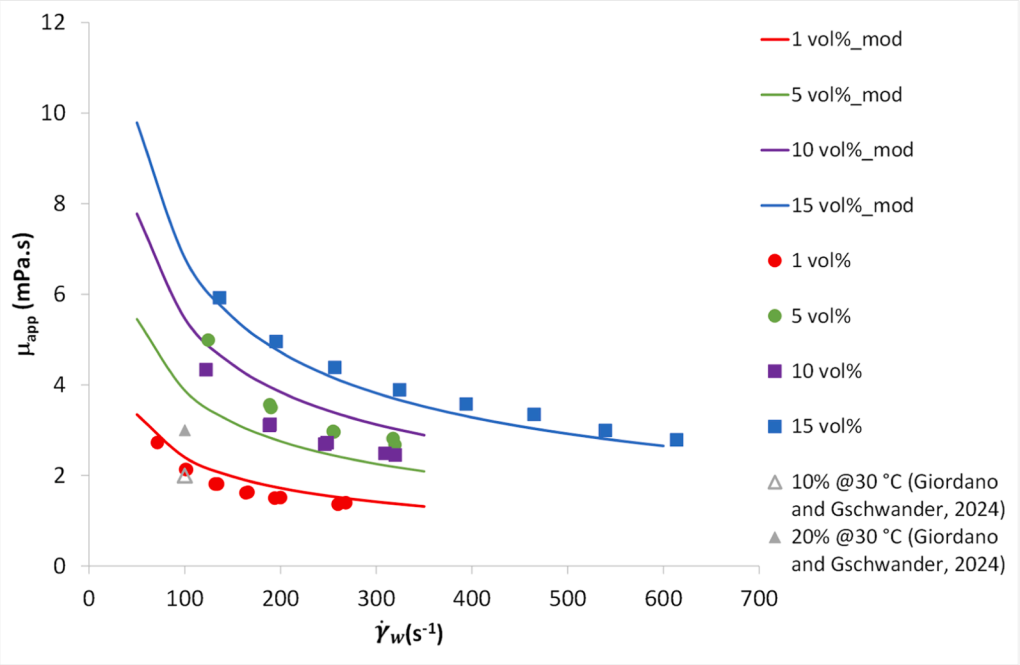


**Fig. 6.** Evolution of the viscosity of emulsions obtained from experimental data (dots) and from model (line) (without AOT at 25 °C).

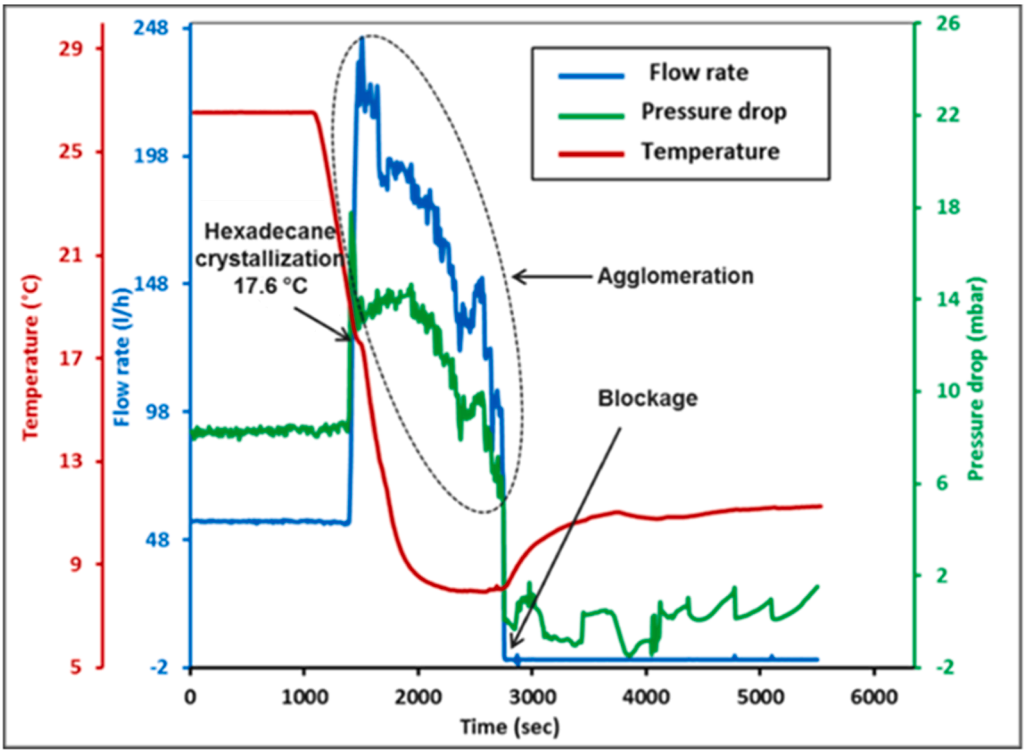


**Fig. 7.** Evolution of pressure drop at various flow rates as function of time of dispersion with 15 vol % of H/W after HD crystallization.

### 3.2. *Emulsion characterization in presence of AOT*

#### 3.2.1. *Effect of AOT on the droplet size of the native emulsions*

AOT is known as anti-agglomerant. Once added to all made emulsion stabilized by CNCs, the mean droplet size of the emulsions was first compared with and without adding AOT. Fig. 8a illustrates the size distribution of emulsions at three oil ratios: 5, 10 and 15 vol % HD. The addition of 0.5 wt % AOT induced a decrease of the size of the droplets for the three HD concentrations as shown on Fig. 8a. For emulsions with 10 and 15 vol %, the addition of AOT induces a slight decrease in droplets size from 15.2 μm to 13.2 μm. This decrease in size is more significant in the emulsion including 5 vol % of HD with an average diameter of 4.5 μm, it is probably because the proportion of AOT compared to that of CNCs and HD is more important in this sample. It was previously shown that AOT can be adsorbed on the surface of cellulose [63], this allows a decrease in the interfacial tension between

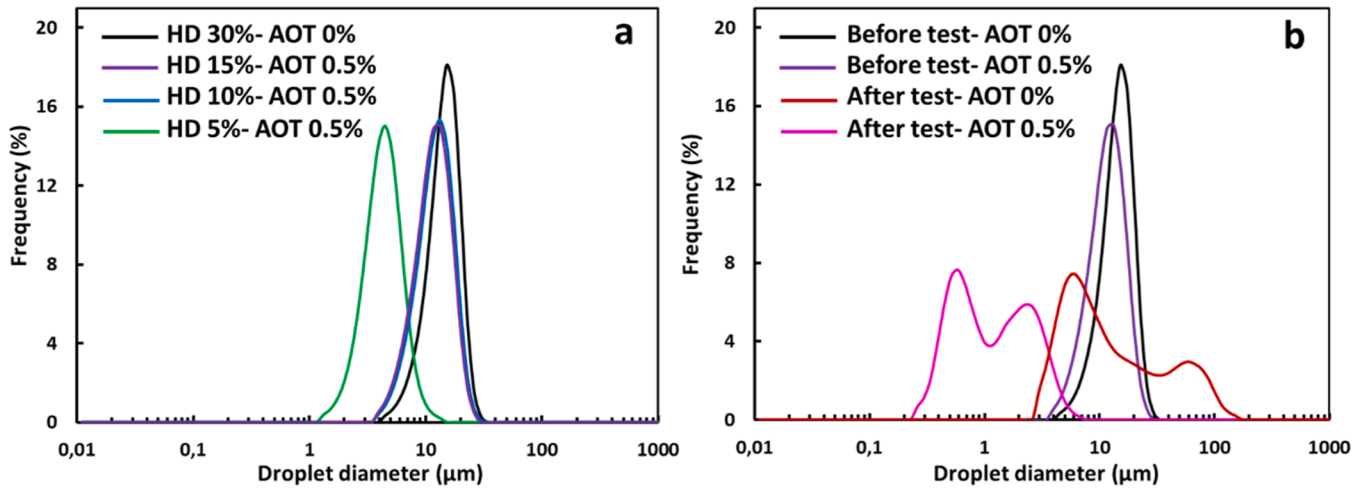


**Fig. 8. a).** Impact of AOT on the distribution of the droplet diameter of the emulsions at different volume fraction of HD and b) Distribution of the average droplet diameter of the 15 vol % H/W emulsion before the rheological test with and without AOT and after the test with and without AOT.

water and oil and an increase in the global interface surface area., we can consider that the decrease in interfacial tension in combination with the increase of interfacial agents brought by AOT can contribute to a decrease in the droplets size.

The impact of AOT on the droplets size after rheological treatment in the solid state of HD was also evaluated. Fig. 8b represents the distribution of droplet diameter of emulsion at 15 vol % of HD before and after use in the loop and after the shearing for emulsion without AOT and with 0.5 wt % AOT. Prior to shearing, the hexadecane droplets diameter was around 15 µm. After shearing the emulsion without AOT, the presence of two droplets populations is observed at approximately 6 µm and 55 µm (Fig. 8b). The decrease in diameter from 15 µm to 6 µm is due to the shearing in the loop, particularly in the pump, as already observed in Jiménez et al. (2018). For these same samples another peak around 55 µm is observed, the presence of this peak corresponds to a coalescence of the droplets, likely caused by continuous shearing, which can compromise the sealing integrity of the droplet surfaces. When AOT is introduced into the emulsion, only a decrease in droplet size from 15 µm to about 4 µm is observed (Fig. 8b). The addition of AOT significantly enhances the droplets stability, avoiding coalescence as previously discussed in the first part of this Section 3.3.1.

### 3.2.2. *Phase change temperature analysis*

As a non-thermodynamic additive, AOT should not alter the phase change temperature of HD. To verify this, DSC analysis was performed. The phase change temperature (PCT) of the various emulsion was found to be around 17.3 and 17.7 °C, and thus the presence of AOT at 0.5 % or 1 % does not change the phase change temperature of the dispersion as given in Table 2. For pure HD, the PCT was given between 17.5 and 18.2 °C [41,43].

## 3.3. *Rheological behaviour of liquid and solid hexadecane dispersion in the loop in presence of AOT*

### 3.3.1. *Flow behaviour of solid HD emulsion containing 0.5 wt% of AOT*

To prevent agglomeration of emulsions circulating in the loop, an antiagglomerant additive (AOT) was added with a concentration of 0.5 wt % for all the samples. Fig. 9 represents the evolution of the pressure drop and the flow rate as a function of time and temperature of the emulsion at 15 vol % of HD in the presence of 0.5 wt % of AOT at 11 °C. In this case, a decrease in flow rate and an increase in pressure drop at 18 °C were observed due to HD crystallization. Indeed, the density of the emulsion decreases after the phase change, as paraffin shrinks upon solidification. Once HD crystallization is complete at 5000 seconds, the flow rate and pressure drop values become stable. Regarding the regular shape of flow rate and pressure drops plateaus, it is obvious that the addition of AOT in the dispersion prevents the hexadecane solid particles agglomeration during rheological measurements.

**Table 2**
PCT of emulsion at 10 vol % of HD obtained by DCS analysis.

| AOT (wt %) | PCT ( °C) |
|---|---|
| 0 | 17.71 |
| 0.5 | 17.35 |
| 1 | 17.38 |

### 3.3.2. *Influence of the HD content on the rheological behaviour of dispersions containing 0.5 wt % of AOT in the solid state of HD*

The rheological behaviours of H/W dispersions at 0.5 wt % of AOT and different HD volume fractions between 0 and 15 vol % circulating in the loop at the solid state oh HD were determined from the experimental data (pressure drop at various flow rates) measured by the capillary viscometer. First, the behaviour index ($n$) of dispersions containing 0 vol %, 5 vol %, 10 vol %, and 15 vol % of HD with 0.5 wt % of AOT determined with experimental data using Eq. (4) is given in Fig. 8a. As observed in the liquid state of HD, all samples exhibit a non-Newtonian fluid with an $n \neq 1$ and the behaviour index is stable for the HD volume fraction between 1 and 15 vol % for both temperatures as shown in Fig. 5a and 10a. This suggests that the dispersion enters a stable pseudoplastic regime, where further increases in HD concentration have little effect on the behaviour index for the tested volume fraction of HD between 0 and 15 vol %. Here also, the yield stress $\tau_0$ can be neglected. The evolution of the consistency index k as a function of HD volume fraction in the solid state is given in Fig. 10b The results indicate that increasing HD volume fraction allows to an increase in the consistency index indicating an increase in the flow resistance and the viscosity of the dispersion.

The apparent viscosities of these same dispersions were then determined with experimental data using Eq. (6) and are given in Fig. 11. We can see that all the dispersions exhibit shear-thinning behaviour, the apparent viscosity decreases by increasing the shear rate. As expected, the viscosity increases with the volume fraction of HD as observed in our previous study [47,64,62].

### 3.3.3. *Influence of the concentration of AOT on the rheological behaviour of dispersion at constant HD volume fraction*

The influence of AOT on the viscosity of dispersion at a constant

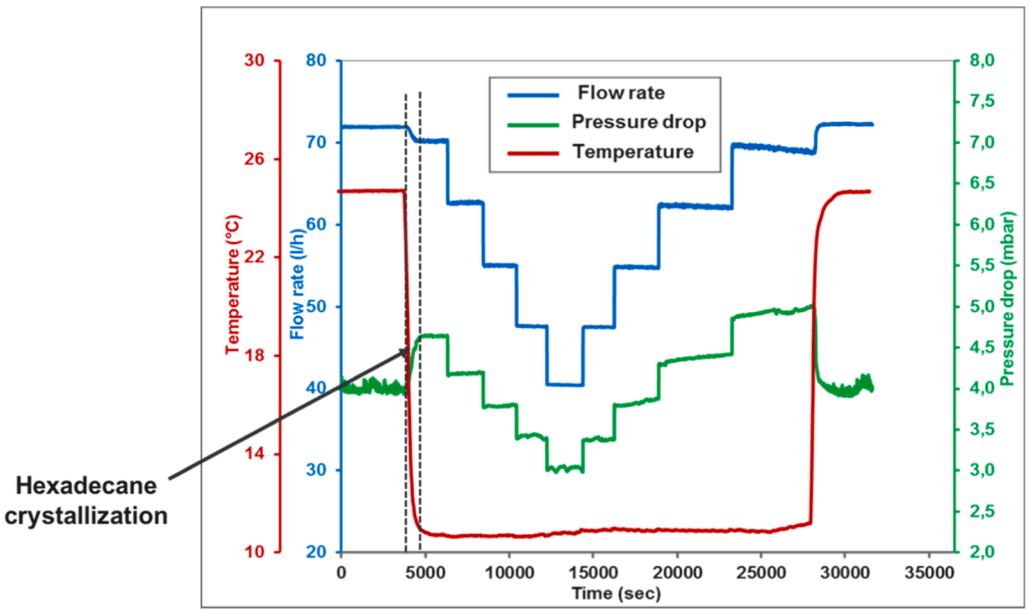


**Fig. 9.** Evolution of pressure drop at various flow rates as a function of time of emulsion at 15 vol % of HD with 0.5 wt % AOT at 11 °C.

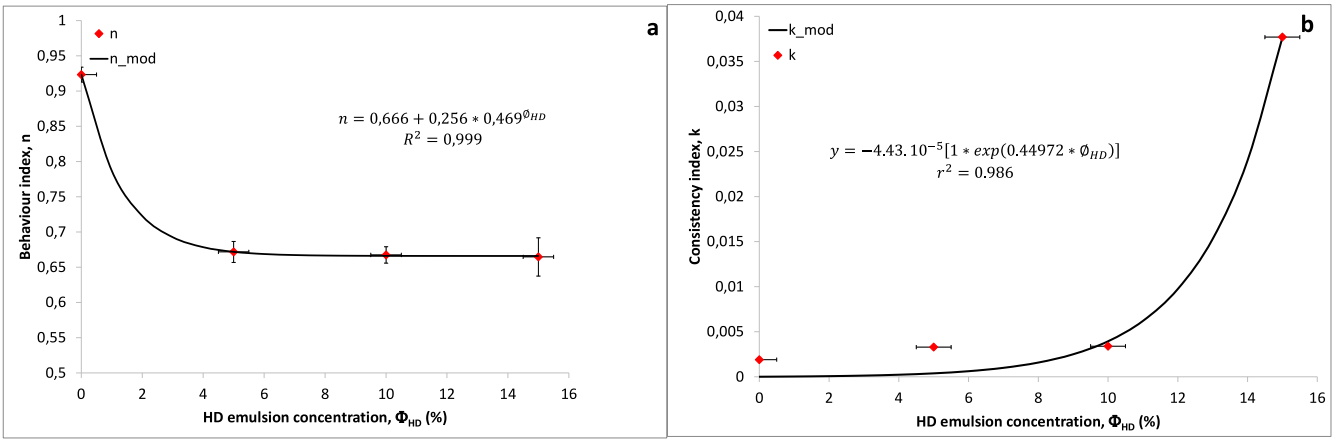


**Fig. 10.** Evolution of a) the behaviour index *n* and b) the consistency index *k* as a function of HD concentration at 0.5 wt % AOT.

volume fraction of HD was then studied. Fig. 12 represent the evolution of the experimental viscosities and viscosities obtained from model of dispersion containing 15 vol % HD at 0.5, 0.75 and 1 wt % of AOT in the solid state of HD (11 °C). It appears that when the AOT concentration is increased from 0.5 % to 0.75 %, a decrease in the dispersion viscosity is observed, which aligns with expectations. However, contrary to what might be anticipated, the viscosity does not decrease when the AOT concentration reaches 1 %. This could be due to the formation of AOT aggregates in the aqueous phase (CMC), leading to an increase in viscosity. Based on these results, it could be interesting to investigate whether there is a correlation between the concentration of HD and AOT in the dispersion.

### 3.3.4. *AOT concentration optimization*

To better understand the effect of AOT on the viscosity of H/W emulsions, the AOT was added in the samples with at different concentration from 0.25 to 1 wt % depending on the volume fraction of HD in the samples from 5 to 20 vol %.

The amount of AOT added in each sample was calculated in relation to the total surface displayed by the HD droplets ($S_d$) in the emulsion (Table 3). The $S_d$ was calculated as described in Cherhal et al. [18].

$$S_d = 4\pi R^2 \times \frac{3V_{HD}}{4\pi R^3} = \frac{3V_{HD}}{R} \quad (9)$$

Where R is the average drop radius and $V_{HD}$ is the volume of HD in the emulsion.

The viscosity of the dispersions with different volume fraction of HD at the optimized AOT concentration were then determined at 11 °C (Fig. 13). As expected, even at the optimal AOT concentration, the viscosity remains high as the HD concentration increases.

Fig. 14 represents a comparative analysis of the rheological behaviour of two different phase change materials (PCMs): $CO_2$ gas hydrates and hexadecane dispersions with AOT. Although these materials are chemically distinct, both systems are regarded as two-phase slurries in secondary refrigeration processes. By studying both materials under identical flow conditions in similar flow loops, direct assessment of how each MCP responds to shear rate is possible and surfactant concentration, as well as the effectiveness assessment of AOT in improving flow properties. An obvious tendency is observed: the apparent viscosity of the slurries increases as a function of the solid fraction. This result is expected and consistent with existing literature [65–68,52]. An interesting observation is the significant improvement in the flow behaviour of both hexadecane and $CO_2$ hydrate slurries with AOT. Without AOT,

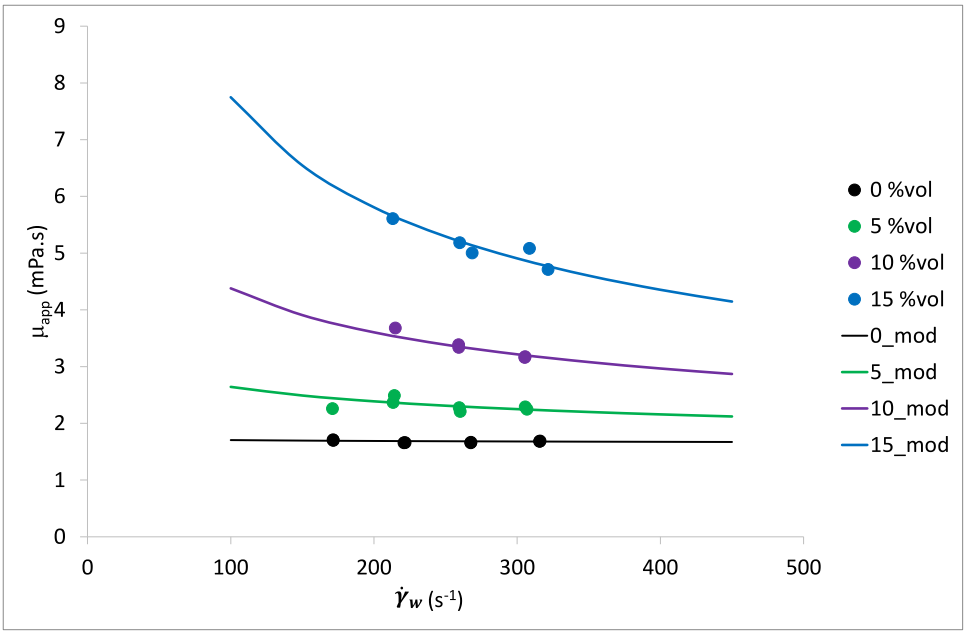


**Fig. 11.** Evolution of the viscosity of dispersions obtained from experimental data (dots) and from model (line) with 0.5 wt % AOT at 11 °C.

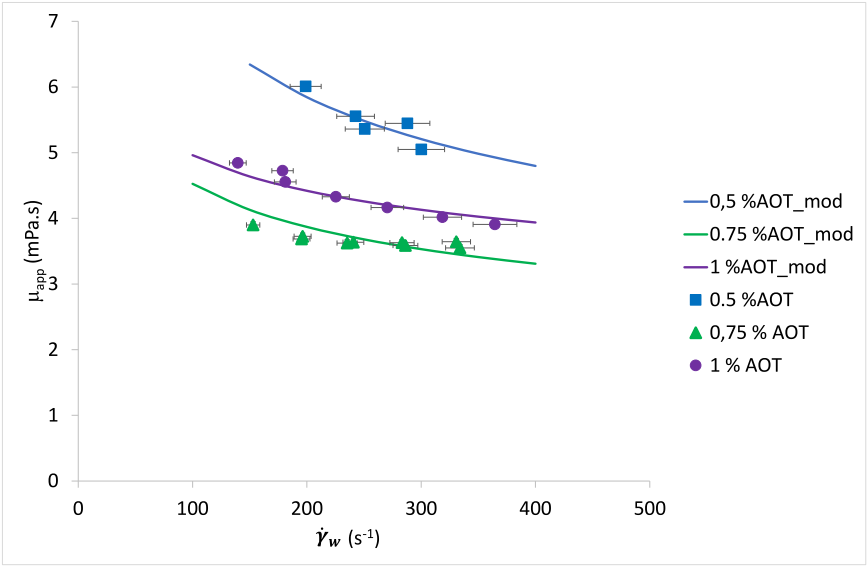


**Fig. 12.** Evolution of the viscosity of dispersions at 15 vol % HD with 0.5, 0.75 and 1 wt % AOT at 10 °C obtained from experimental data (dots) and from model (line).

**Table 3**
Determination of the AOT concentration depending on the HD volume fraction.

| Hexadecane (vol %) | Total surface of oil droplets ($m^2$) | AOT (wt %) |
|---|---|---|
| 5 | 150 | 0.25 |
| 10 | 300 | 0.5 |
| 15 | 450 | 0.75 |
| 20 | 600 | 1 |

the viscosity of the HD slurry increases quickly with the solid fraction, indicating the formation of particle agglomerates as seen in Section 3.3.2. However, when AOT is introduced, the increase in viscosity with solid fraction is much less pronounced. An additional key observation is that the overall apparent viscosity increases with higher AOT concentrations for both types of slurries but is still acceptable for the targeted application in the case of H/W dispersion. For example, with 10 vol % HD and 1 wt % AOT, the apparent viscosity is about 4 mPa·s. In $CO_2$ hydrate slurries, the viscosity values are nearly twice as high as those found in H/W dispersions at the same AOT concentration and solid fraction. This effect can be understood by looking at the structural difference between the two slurries. $CO_2$ hydrates likely possess a more rigid crystalline structure, which contributes to a strong flow resistance and, in turn, a higher apparent viscosity. HD slurry exhibits lower viscosity because its droplets can deform more easily. This ability to change shape under shear reduces friction and facilitates smoother flow.

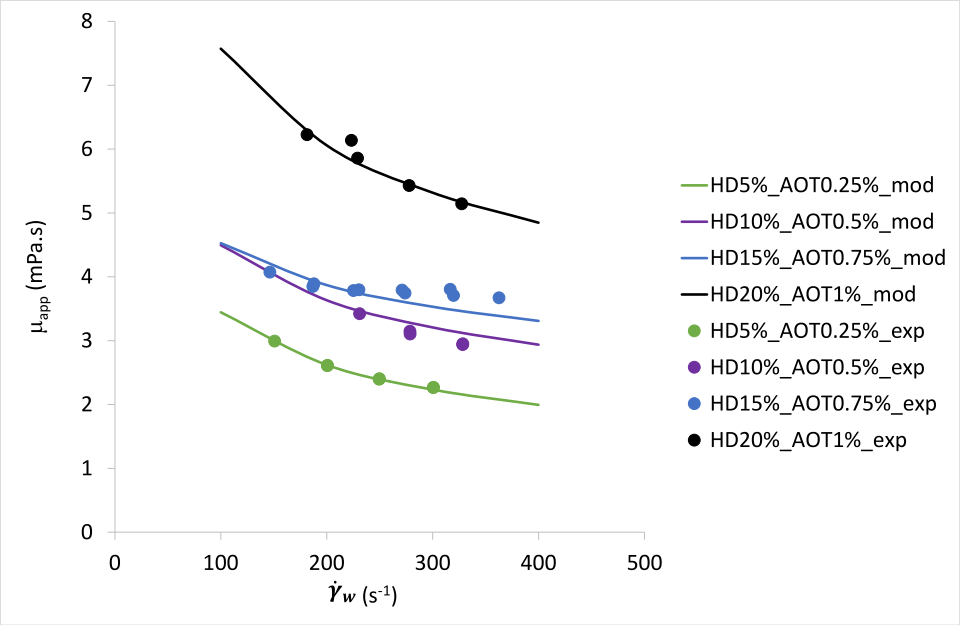


**Fig. 13.** Evolution of the viscosity of H/Wdispersions containing 5, 10, 15 and 20 vol % of HD at 0.25, 0.5, 0.75 and 1 wt % of AOT respectively at 11 °C obtained from experimental data (dots) and from model (line).

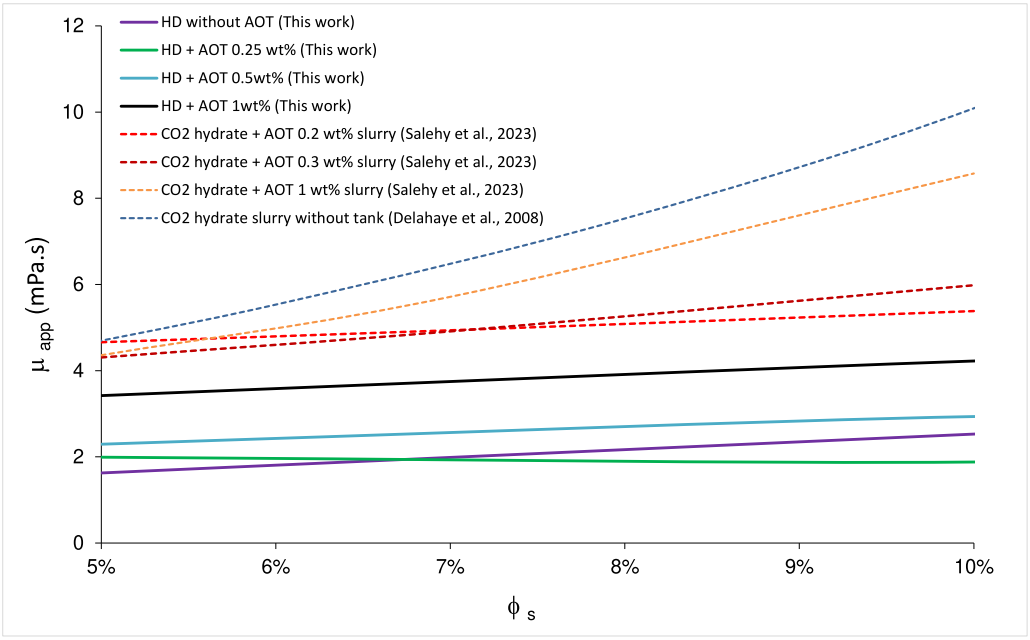


**Fig. 14.** Comparison of the apparent viscosities of various phase-change material slurries with and without AOT on the same experimental loop at 400 $s^{-1}$.

### *3.4. Influence of the cycling (shearing in the loop) on the viscosity of dispersions containing 15 vol% of HD and 0.5 wt% of AOT at the solid and liquid state of HD*

The viscosity of the dispersions subjected to cooling/heating cycles under shear was measured. First, the viscosity as a function of shear rate was determined for the dispersion circulating in the loop at 25 °C. The sample temperature was then lowered to 11 °C, and after temperature stabilization, the viscosity as a function of shear rate was then determined at 11 °C. During the cooling/heating cycles the HD droplets in water underwent repeated liquid-solid and solid-liquid phase change over 10 times.

Fig. 15 represents the viscosities at 25 °C and 11 °C for an dispersion with 15 vol % HD and 0.5 wt % AOT. The results indicated a shear thinning behaviour at both temperatures. The viscosity of the dispersion in the solid state is consistently higher than that in its liquid state, as observed in the literature [61]: this phenomenon can be explained by difference in the deformability of HD particles depending on the temperature. Specifically, solid droplets deform minimally under shear stress, which makes it difficult for the dispersion to flow through different sections of the loop and generating then more friction at the walls, leading to a higher pressure drop and increase in viscosity when the paraffin is solidified. In contrast, liquid droplets can deform significantly, allowing them to flow more easily in the loop as observed in literature [64,61]

We also observed in Fig. 15 that between the first and the second

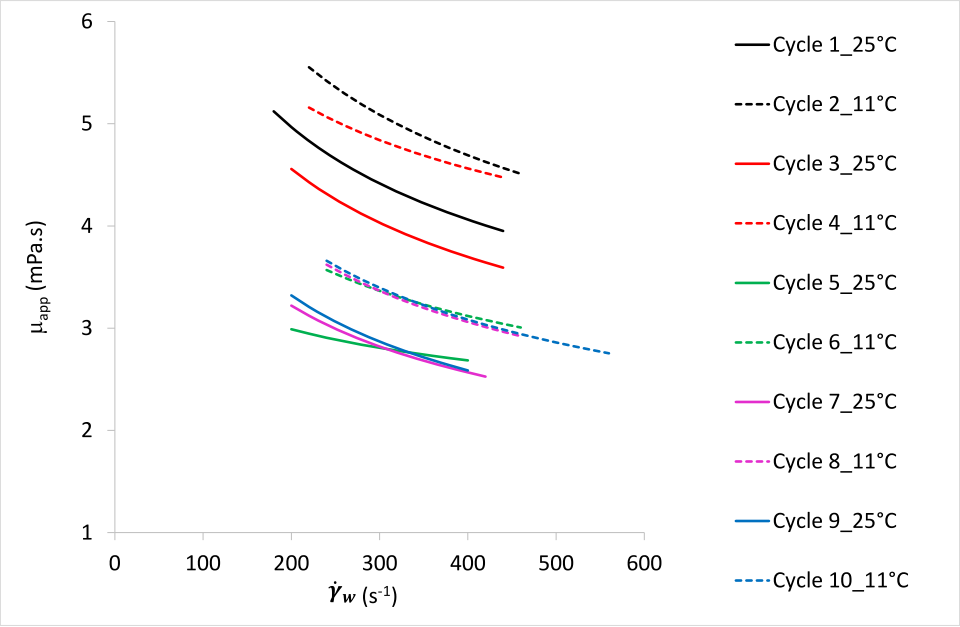


**Fig. 15.** Viscosity at 25 °C (line) and 11 °C (dash) of dispersion with 15 vol % of HD and 0.5 wt % of AOT before and after cooling/heating cycles in the loop.

cycle, the viscosity decreases by about 10% for both states, and by 25% between the second and third cycle. Beyond the third cycle, the viscosities remain of the same order of magnitude. An explanation could be linked to the evolution of droplets size wich was verified over the cycles. Fig. 16 represents the distrubtion of the droplets size of dispersion containing 15 vol % of HD at 0.5 wt % of AOT before and after the cooling/heating cycles in the loop.

The droplet sizes of the emulsion before and after the cooling/heating cycles under shear rates are given in Fig. 16. A noticeable decreasing in droplet size is observed following the shear cycles in the loop. Unlike the emulsion without treatment where the size distribution is centered around 15 μm, the emulsion after the cycles (4 and 10) represents two populations of droplet sizes at about 4 μm and 0.4 μm. This decrease is linked to the presence of AOT under shear rate as discussed earlier in Section (3.1.). We therefore note that the viscosity of the emulsions could be correlated to the droplets size, the smaller the droplets, the lower the viscosity as already observed in our previous work. The decrease in size is also confirmed by the microscopic observations shown in Fig. 17. Interestingly, while the viscosity stabilizes after the fourth cycle, the droplet size continues to decrease. We

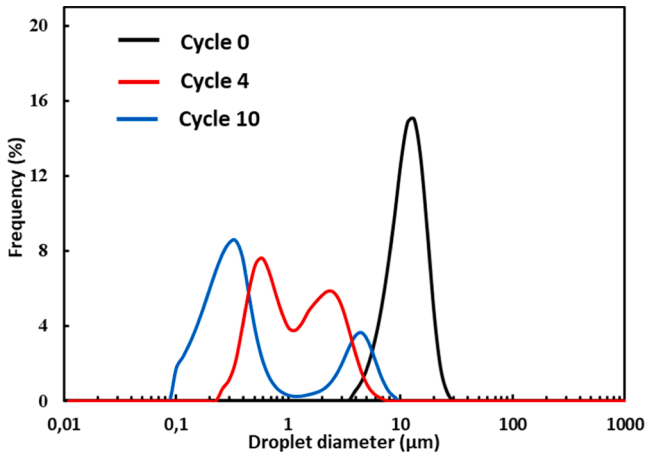


**Fig. 16.** Distribution of the average droplet diameter of emulsion with 15 vol % of HD and 0.5 wt % of AOT before and after cooling/heating cycles in the loop.

assumed that the reduction of the viscosity is dominantly driven by the mechanical interaction of the gear pump, which repeatedly shear the emulsions or dispersions under high shear rate. Every successive pass through the pump causes a further destruction of the droplets until the droplets are reduced to a size where there is no longer significant deformation or breakup of the droplets by the shear field inside the gear teeth. This suggests that beyond a certain droplet size, viscosity is no longer affected.

## Conclusion

This study provides a comprehensive analysis of the rheological behaviour, droplet size evolution and flow behaviour of hexadecane-in-water emulsions stabilized by cellulose nanocrystals (CNCs) and AOT in a flow loop. Our results demonstrated that AOT plays a key role in reducing droplet size, especially at lower hexadecane concentrations, by stabilizing the oil-water interface and preventing coalescence. Importantly, AOT did not affect the phase change temperature of hexadecane, confirming its non-thermodynamic nature. Rheological analyses showed that the emulsions exhibit shear-thinning behaviour, with viscosity increasing alongside hexadecane concentration. The introduction of AOT effectively prevented the agglomeration of solid HD particles, ensuring stable flow conditions and consistent pressure drops during the flow. Moreover, a direct observation between smaller droplet sizes and lower viscosity was observed. When the droplet size distribution continues to decrease over the thermal cycles the apparent viscosity stabilized from the third cycle. These findings contribute to the development of energy-efficient refrigeration systems utilizing phase change material slurries. By optimizing AOT concentrations, it is possible to achieve emulsions with improved flow characteristics, reduced viscosity, and enhanced stability during phase transitions. Further investigation must be carried out to ensure the long-term stability of these emulsions under continuous operating conditions and the potential formation of AOT aggregates at higher concentrations, as well as the impact of shear rate on droplet size control, which could affect viscosity in unexpected ways.

## CRediT authorship contribution statement

**Pascal Clain:** Writing – review & editing, Writing – original draft, Visualization, Software, Methodology, Investigation, Data curation.

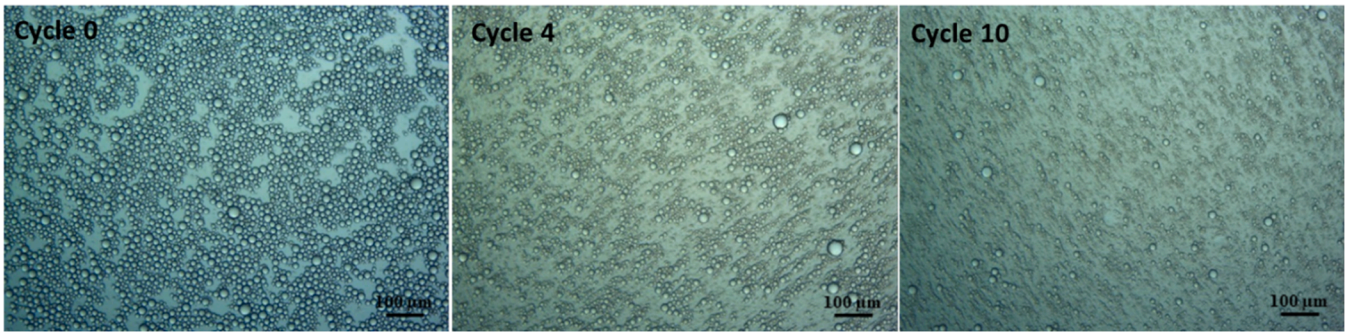


**Fig. 17.** Microscopy images of emulsion containing 15 vol % HD before and after cooling/heating cycles at 0.5 wt % AOT.

**Somia Haouache:** Writing – review & editing, Writing – original draft, Visualization, Software, Methodology, Investigation, Data curation. **Isabelle Capron:** Writing – review & editing, Validation, Supervision, Resources, Project administration. **Anthony Delahaye:** Writing – review & editing, Validation, Supervision, Resources, Methodology, Conceptualization. **Laurence Fournaison:** Writing – review & editing, Visualization, Validation, Supervision, Project administration.

## Declaration of competing interest

The authors declare that they have no known competing financial interests or personal relationships that could have appeared to influence the work reported in this paper.

## Appendix A. Absolute uncertainty of rheological behaviour of liquid HD emulsion without AOT.

| Hexadecane fraction, $\Phi_{HD}$ ( %) | $\Phi_{HD}$ absolute uncertainty | Behaviour index, n | Absolute Behaviour index uncertainty | Consistency index, k | Absolute consistency index uncertainty |
|---|---|---|---|---|---|
| 0 | ±0 | 1 | ±0 | 0,0013 | ±5,896E-06 |
| 1 | ±0,5 | 0,55 | ±0,0095 | 0,0172 | ±0000,256 |
| 5 | ±0,5 | 0,51 | ±0,0158 | 0,0652 | ±0,0016 |
| 10 | ±0,5 | 0,42 | ±0,0102 | 0046 | ±0,0014 |
| 15 | ±0,5 | 0,52 | ±0,0126 | 0,0678 | ±0,0022 |

| $\Phi_{HD}$ ( %) | Shear rate, $\dot{\gamma}_w$ ($s^{-1}$) | Absolute shear rate uncertainty ($s^{-1}$) | Apparent viscosity (mPa.s) | Absolute apparent viscosity uncertainty (mPa.s) |
|---|---|---|---|---|
| 0 | 280 | ±1,3 | 1,5 | ±0,0151 |
| 0 | 234 | ±1,3 | 1,4 | ±0015 |
| 0 | 186 | ±1,3 | 1,4 | ±0,0168 |
| 0 | 135 | ±1,3 | 1,5 | ±0,0214 |
| 0 | 136 | ±1,3 | 1,5 | ±0,0213 |
| 0 | 182 | ±1,3 | 1,4 | ±0,0171 |
| 0 | 234 | ±1,3 | 1,4 | ±0,0150 |
| 0 | 281 | ±1,3 | 1,5 | ±0,0153 |
| 1 | 262 | ±2,2 | 1,4 | ±0,0174 |
| 1 | 196 | ±1,6 | 1,5 | ±0,0194 |
| 1 | 162 | ±1,3 | 1,7 | ±0,0214 |
| 1 | 131 | ±1,1 | 1,9 | ±0,0243 |
| 1 | 100 | ±0,8 | 2,2 | ±0,0294 |
| 1 | 99 | ±0,8 | 2,2 | ±0,0295 |
| 1 | 129 | ±1,1 | 1,9 | ±0,0244 |
| 1 | 160 | ±1,3 | 1,7 | ±0,0213 |
| 1 | 190 | ±1,6 | 1,5 | ±0,0194 |
| 1 | 254 | ±2,1 | 1,4 | ±0,0171 |
| 5 | 319 | ±4,2 | 2,7 | ±0,0418 |
| 5 | 255 | ±3,7 | 3 | ±0,0499 |
| 5 | 189 | ±2,9 | 3,6 | ±0,0617 |
| 5 | 190 | ±2,6 | 3,5 | ±0,0557 |
| 5 | 256 | ±3,2 | 3 | ±0,0449 |
| 5 | 317 | ±3,9 | 2,8 | ±0,0419 |
| 10 | 341 | ±4,0 | 2,3 | ±0,0331 |
| 10 | 265 | ±3,1 | 2,6 | ±0,0369 |
| 10 | 201 | ±2,4 | 2,9 | ±0,0426 |
| 10 | 130 | ±1,5 | 4,1 | ±0,0592 |
| 10 | 201 | ±2,4 | 2,9 | ±0,0422 |
| 10 | 262 | ±3,1 | 2,5 | ±0,0364 |
| 10 | 329 | ±3,9 | 2,3 | ±0,0336 |
| 15 | 316 | ±2,2 | 4,0 | ±0,0425 |
| 15 | 250 | ±1,7 | 4,5 | ±0048 |
| 15 | 190 | ±1,3 | 5,1 | ±0,0544 |

(*continued on next page*)

(*continued*)

| $\Phi_{HD}$ ( %) | Shear rate, $\dot{\gamma}_w$ ($s^{-1}$) | Absolute shear rate uncertainty ($s^{-1}$) | Apparent viscosity (mPa.s) | Absolute apparent viscosity uncertainty (mPa.s) |
|---|---|---|---|---|
| 15 | 133 | ±0,9 | 6,1 | ±0065 |
| 15 | 597 | ±4,1 | 2,9 | ±0,0303 |
| 15 | 525 | ±3,6 | 3,1 | ±0,0326 |
| 15 | 453 | ±3,1 | 3,4 | ±0,0365 |
| 15 | 384 | ±2,7 | 3,7 | ±0,0390 |

## Appendix B. : Absolute uncertainty of rheological behaviour solid HD emulsion containing 0.5 wt % of AOT.

| Hexadecane fraction, $\Phi_{HD}$ ( %) | $\Phi_{HD}$ absolute uncertainty | Behaviour index, n | Absolute Behaviour index uncertainty | Consistency index, k | Absolute consistency index uncertainty |
|---|---|---|---|---|---|
| 0 | 0 | 0,92 | ±0011 | 0,0019 | ±0000,012 |
| 1 | ±0,5 | 0,67 | ±0015 | 0,0033 | ±0000,073 |
| 5 | ±0,5 | 0,67 | ±0012 | 0,0034 | ±0000,082 |
| 10 | ±0,5 | 0,66 | ±0,0271 | 0,0377 | ±0000,146 |
| 15 | ±0,5 | 0,92 | ±0,0106 | 0,0019 | ±0000,012 |

| $\Phi_{HD}$ ( %) | Shear rate, $\dot{\gamma}_w$ ($s^{-1}$) | Absolute shear rate uncertainty ($s^{-1}$) | Apparent viscosity (mPa.s) | Absolute apparent viscosity uncertainty (mPa.s) |
|---|---|---|---|---|
| 0 | 316 | ±1,7 | 1,7 | ±0,0165 |
| 0 | 268 | ±1,7 | 1,7 | ±0,0175 |
| 0 | 222 | ±1,4 | 1,7 | ±0,0179 |
| 0 | 172 | ±1,1 | 1,7 | ±0,0195 |
| 0 | 172 | ±0,7 | 1,7 | ±0,0206 |
| 0 | 221 | ±0,7 | 1,7 | ±0,0205 |
| 0 | 268 | ±0,9 | 1,7 | ±0,0182 |
| 0 | 316 | ±1,2 | 1,7 | ±0017 |
| 5 | 307 | ±1,5 | 2,2 | ±0,0202 |
| 5 | 260 | ±1,2 | 2,2 | ±0,0217 |
| 5 | 214 | ±1 | 2,5 | ±0,0237 |
| 5 | 171 | ±0,7 | 2,3 | ±0,0275 |
| 5 | 213 | ±1 | 2,4 | ±0,0239 |
| 5 | 260 | ±1,2 | 2,3 | ±0022 |
| 5 | 306 | ±1,5 | 2,3 | ±0,0207 |
| 10 | 305 | ±2,5 | 3,2 | ±0,0276 |
| 10 | 259 | ±2,2 | 3,4 | ±0,0279 |
| 10 | 215 | ±2 | 3,7 | ±0,0289 |
| 10 | 259 | ±1,7 | 3,3 | ±0,0304 |
| 10 | 306 | ±1,4 | 3,2 | ±0,0328 |
| 15 | 322 | ±2,3 | 4,7 | ±0,0288 |
| 15 | 269 | ±2 | 5,0 | ±0,0307 |
| 15 | 213 | ±1,7 | 5,6 | ±0,0318 |
| 15 | 260 | ±1,5 | 5,2 | ±0,0337 |
| 15 | 309 | ±1,9 | 5,1 | ±0,0312 |

## Appendix C. : Absolute uncertainty of rheological behaviour solid 15 vol % HD emulsion containing AOT.

| $\Phi_{AOT}$ ( %) | $\Phi_{AOT}$ absolute uncertainty | Shear rate, $\dot{\gamma}_w$ ($s^{-1}$) | Absolute shear rate uncertainty ($s^{-1}$) | Apparent viscosity (mPa.s) | Absolute apparent viscosity uncertainty (mPa.s) |
|---|---|---|---|---|---|
| 0,5 | 0,05 | 300 | ±20,4 | 5,0 | ±0,3451 |
| 0,5 | 0,05 | 251 | ±17,1 | 5,4 | ±0,3675 |
| 0,5 | 0,05 | 199 | ±13,5 | 6,0 | ±0,4121 |
| 0,5 | 0,05 | 243 | ±16,5 | 5,6 | ±0,3796 |
| 0,5 | 0,05 | 288 | ±19,5 | 5,4 | ±0,3718 |
| 0,75 | 0,05 | 334 | ±12,6 | 3,6 | ±0,1373 |
| 0,75 | 0,05 | 286 | ±10,9 | 3,6 | ±0,1393 |
| 0,75 | 0,05 | 241 | ±9,1 | 3,6 | ±0,1412 |
| 0,75 | 0,05 | 196 | ±7,5 | 3,7 | ±0,1448 |
| 0,75 | 0,05 | 153 | ±5,8 | 3,9 | ±0,1516 |
| 0,75 | 0,05 | 195 | ±7,4 | 3,7 | ±0,1427 |
| 0,75 | 0,05 | 235 | ±8,8 | 3,6 | ±0,1394 |
| 0,75 | 0,05 | 283 | ±10,6 | 3,6 | ±0,1393 |
| 0,75 | 0,05 | 331 | ±12,4 | 3,6 | ±0,1397 |
| 1 | 0,05 | 364 | ±19,2 | 3,9 | ±0,2078 |
| 1 | 0,05 | 319 | ±16,8 | 4,0 | ±0,2137 |
| 1 | 0,05 | 270 | ±14,2 | 4,2 | ±0,2216 |
| 1 | 0,05 | 225 | ±11,8 | 4,3 | ±0,2302 |
| 1 | 0,05 | 181 | ±9,5 | 4,6 | ±0,2422 |

(*continued on next page*)

(*continued*)

| $\Phi_{AOT}$ ( %) | $\Phi_{AOT}$ absolute uncertainty | Shear rate, $\dot{\gamma}_w$ ($s^{-1}$) | Absolute shear rate uncertainty ($s^{-1}$) | Apparent viscosity (mPa.s) | Absolute apparent viscosity uncertainty (mPa.s) |
|---|---|---|---|---|---|
| 1 | 0,05 | 140 | ±7,3 | 4,8 | ±0,2578 |
| 1 | 0,05 | 179 | ±9,4 | 4,7 | ±0,2507 |

## Appendix D. : Absolute uncertainty of rheological behaviour at 25 °C and 11 °C of dispersion with 15 vol % of HD and 0.5 wt % of AOT.

| Cycle | Shear rate, $\dot{\gamma}_w$ ($s^{-1}$) | Absolute shear rate uncertainty ($s^{-1}$) | Apparent viscosity (mPa.s) | Absolute apparent viscosity uncertainty (mPa.s) |
|---|---|---|---|---|
| 1 | 357 | ±3,2 | 4,2 | ±0,0506 |
| 1 | 308 | ±2,8 | 4,4 | ±0,0528 |
| 1 | 262 | ±2,4 | 4,5 | ±0055 |
| 1 | 215 | ±1,9 | 4,9 | ±0,0593 |
| 1 | 213 | ±1,9 | 4,9 | ±0,0596 |
| 1 | 263 | ±2,4 | 4,6 | ±0,0553 |
| 1 | 310 | ±2,8 | 4,4 | ±0053 |
| 1 | 361 | ±3,9 | 4,2 | ±0,0512 |
| 1 | 334 | ±5,4 | 3,8 | ±0,0688 |
| 1 | 283 | ±4,6 | 4,0 | ±0,0723 |
| 1 | 233 | ±3,8 | 4,3 | ±0,0783 |
| 1 | 282 | ±4,6 | 4,1 | ±0,0738 |
| 3 | 334 | ±5,4 | 3,8 | ±0,0688 |
| 3 | 310 | ±3,7 | 2,7 | ±0,0397 |
| 3 | 262 | ±3,2 | 2,8 | ±0,0407 |
| 3 | 216 | ±2,6 | 2,9 | ±0,0429 |
| 3 | 262 | ±3,2 | 2,8 | ±0,0415 |
| 5 | 311 | ±3,7 | 2,8 | ±0040 |
| 5 | 343 | ±6,0 | 2,7 | ±0,0521 |
| 5 | 289 | ±5,1 | 2,8 | ±0,0545 |
| 5 | 238 | ±4,2 | 3,0 | ±0,0589 |
| 5 | 289 | ±5,1 | 2,7 | ±0,0518 |
| 7 | 342 | ±6,0 | 2,5 | ±0,0493 |
| 7 | 357 | ±7,3 | 2,6 | ±0,0568 |
| 7 | 301 | ±6,1 | 2,8 | ±0,0605 |
| 7 | 247 | ±5,0 | 3,0 | ±0,0657 |
| 7 | 300 | ±6,1 | 2,5 | ±0056 |
| 9 | 356 | ±7,3 | 2,4 | ±0,0537 |
| 9 | 357 | ±3,2 | 4,2 | ±0,0506 |
| 9 | 308 | ±2,8 | 4,4 | ±0,0528 |
| 9 | 262 | ±2,4 | 4,5 | ±0055 |
| 9 | 215 | ±1,9 | 4,9 | ±0,0593 |
| 2 | 310 | ±4,7 | 4,9 | ±0,0832 |
| 2 | 259 | ±3,9 | 5,2 | ±0,0883 |
| 2 | 206 | ±3,1 | 5,8 | ±0,0991 |
| 2 | 251 | ±3,8 | 5,4 | ±0,0915 |
| 2 | 298 | ±4,5 | 5,3 | ±0,0897 |
| 4 | 301 | ±7,3 | 4,6 | ±0,1177 |
| 4 | 255 | ±6,2 | 4,9 | ±0,1265 |
| 4 | 254 | ±6,2 | 4,9 | ±0,1251 |
| 4 | 301 | ±7,3 | 4,7 | ±0,1219 |
| 6 | 363 | ±5,6 | 3,2 | ±0,0555 |
| 6 | 314 | ±4,8 | 3,3 | ±0,0579 |
| 6 | 267 | ±4,1 | 3,5 | ±0,0604 |
| 6 | 313 | ±4,8 | 3,3 | ±0,0574 |
| 6 | 362 | ±5,5 | 3,3 | ±0,0563 |
| 8 | 376 | ±6,6 | 3,1 | ±0,0601 |
| 8 | 325 | ±5,7 | 3,3 | ±0,0641 |
| 8 | 276 | ±4,9 | 3,4 | ±0,0669 |
| 8 | 324 | ±5,7 | 3,2 | ±0,0615 |
| 8 | 375 | ±6,6 | 3,1 | ±0,0606 |
| 10 | 376 | ±6,7 | 3,2 | ±0,0627 |
| 10 | 325 | ±5,8 | 3,3 | ±0,0649 |
| 10 | 277 | ±4,9 | 3,5 | ±0,0685 |
| 10 | 324 | ±5,8 | 3,2 | ±0,0621 |
| 10 | 374 | ±6,7 | 3,1 | ±0,0605 |

## Data availability

Data will be made available on request.

## References

[1] International Institute of Refrigeration, 2015. The role of refrigeration in the global economy. 29th informatory note on refrigeration technologies. [WWW Document]. URL https://sainttrofee.nl/wp-content/uploads/2019/01/NoteTech_29-World-Statistics.pdf (accessed 11.27.24).

[2] C.I.P. Martínez, A.C. Poveda, Challenges and opportunities in the management of refrigeration and air conditioning systems to reduce environmental impacts in the Colombian health sector, Int. J. Refrig. 141 (2022) 54–65.
[3] L. Huang, M. Petermann, C. Doetsch, Evaluation of paraffin/water emulsion as a phase change slurry for cooling applications, Energy 34 (2009) 1145–1155.
[4] J. Shao, J. Darkwa, G. Kokogiannakis, Development of a novel phase change material emulsion for cooling systems, Renew. Energy 87 (2016) 509–516.
[5] V. Vasile, H. Necula, A. Badea, R. Revellin, J. Bonjour, P. Haberschill, Experimental study of the heat transfer characteristics of a paraffin-in-water emulsion used as a secondary refrigerant, Int. J. Refrig. 88 (2018) 1–7.
[6] Z. Youssef, A. Delahaye, L. Huang, F. Trinquet, L. Fournaison, C. Pollerberg, C. Doetsch, State of the art on phase change material slurries, Energy Convers. Manag. 65 (2013) 120–132, https://doi.org/10.1016/j.enconman.2012.07.004.
[7] J. Frelichowska, M.-A. Bolzinger, J.-P. Valour, H. Mouaziz, J. Pelletier, Y. Chevalier, Pickering w/o emulsions: drug release and topical delivery, Int. J. Pharm. 368 (2009) 7–15.
[8] L.L. Schramm, Fundamentals and applications in the petroleum industry, Adv. Chem. 231 (1992) 3–24.
[9] S. Stiller, H. Gers-Barlag, M. Lergenmueller, F. Pflücker, J. Schulz, K.P. Wittern, R. Daniels, Investigation of the stability in emulsions stabilized with different surface modified titanium dioxides, Colloids Surf. Physicochem. Eng. Asp. 232 (2004) 261–267.
[10] A. Timgren, M. Rayner, M. Sjöö, P. Dejmek, Starch particles for food based pickering emulsions, Procedia Food Sci. 1 (2011) 95–103.
[11] S.U. Pickering, Cxcvi.—emulsions, J. Chem. Soc. Trans. 91 (1907) 2001–2021.
[12] W. Ramsden, Separation of solids in the surface-layers of solutions and 'suspensions'(observations on surface-membranes, bubbles, emulsions, and mechanical coagulation).—preliminary account, Proc. R. Soc. L. 72 (1904) 156–164.
[13] G. D'Agostino, M.R. Caruso, G. Cavallaro, G. Lazzara, S. Milioto, Pickering emulsion gel based on funori biopolymer and halloysite nanotubes: a new sustainable material for the cleaning of artwork surfaces, ACS Appl. Polym. Mater. (2024), https://doi.org/10.1021/acsapm.4c01152.
[14] S. Saber, M. Zargartalebi, A. Kazemi, D. Sinton, Pickering phase change slurries, J. Colloid Interface Sci. (2023), https://doi.org/10.1016/j.jcis.2023.07.187.
[15] K.P. Oza, S.G. Frank, MIcrocrystalline cellulose stabilizedemulsions, J. Dispers. Sci. Technol. 7 (1986) 543–561.
[16] C. Jiménez Saelices, I. Capron, Design of pickering micro-and nanoemulsions based on the structural characteristics of nanocelluloses, Biomacromolecules 19 (2018) 460–469.
[17] T. Winuprasith, M. Suphantharika, Properties and stability of oil-in-water emulsions stabilized by microfibrillated cellulose from mangosteen rind, Food Hydrocoll. 43 (2015) 690–699, https://doi.org/10.1016/j.foodhyd.2014.07.027.
[18] F. Cherhal, F. Cousin, I. Capron, Structural description of the interface of pickering emulsions stabilized by cellulose nanocrystals, Biomacromolecules 17 (2016 a) 496–502.
[19] I. Kalashnikova, H. Bizot, B. Cathala, I. Capron, Modulation of cellulose nanocrystals amphiphilic properties to stabilize oil/water interface, Biomacromolecules 13 (2012) 267–275.
[20] I. Kalashnikova, H. Bizot, B. Cathala, I. Capron, New pickering emulsions stabilized by bacterial cellulose nanocrystals, Langmuir 27 (2011) 7471–7479.
[21] T.F. Tadros, Correlation of viscoelastic properties of stable and flocculated suspensions with their interparticle interactions, Adv. Colloid Interface Sci. 68 (1996) 97–200.
[22] T.F. Tadros, Fundamental principles of emulsion rheology and their applications, Colloids Surf. Physicochem. Eng. Asp. 91 (1994) 39–55.
[23] H.A. Barnes, Rheology of emulsions—a review, Colloids Surf. Physicochem. Eng. Asp. 91 (1994) 89–95.
[24] B.P. Binks, J.H. Clint, C.P. Whitby, Rheological Behavior of Water-in-Oil Emulsions Stabilized by Hydrophobic Bentonite Particles, Langmuir 21 (2005) 5307–5316, https://doi.org/10.1021/la050255w.
[25] P.K. Jha, V. Mahto, V.K. Saxena, Study the effect of polymers on the stability and rheological properties of oil-in-water (O/W) Pickering emulsion muds, Korea Aust. Rheol. J. 30 (2018) 127–136, https://doi.org/10.1007/s13367-018-0013-y.
[26] P. Kundu, V. Kumar, I.M. Mishra, Modeling the steady-shear rheological behavior of dilute to highly concentrated oil-in-water (o/w) emulsions: Effect of temperature, oil volume fraction and anionic surfactant concentration, J. Pet. Sci. Eng. 129 (2015) 189–204, https://doi.org/10.1016/j.petrol.2015.03.008.
[27] H. Wang, P.B. Zetterlund, C. Boyer, B.J. Boyd, T.J. Atherton, P.T. Spicer, Large Hexosomes from Emulsion Droplets: Particle Shape and Mesostructure Control, Langmuir 34 (2018) 13662–13671, https://doi.org/10.1021/acs.langmuir.8b02638.
[28] L.L. Schramm, Emulsions, Foams, and Suspensions: Fundamentals and Applications, John Wiley & Sons, 2006.
[29] R. Pal, Effect of droplet size on the rheology of emulsions, AIChE J. 42 (1996) 3181–3190.
[30] S. Abramov, A. Berndt, K. Georgieva, P. Ruppik, H.P. Schuchmann, Investigation of the influence of mean droplet size and shear rate on crystallization behavior of hexadecane-in-water dispersions, Colloids Surf. Physicochem. Eng. Asp. 529 (2017) 513–522.
[31] A.K. Das, D. Mukesh, V. Swayambunathan, D.D. Kotkar, P.K. Ghosh, Concentrated emulsions. 3. Studies on the influence of continuous-phase viscosity, volume fraction, droplet size, and temperature on emulsion viscosity, Langmuir 8 (1992) 2427–2436.
[32] E.S. Rajagopal, Effect of particle size and interfacial film on the viscosity of disperse systems, Z. Phys. Chem. 23 (1960) 342–347.
[33] Y. Salehy, P. Clain, A. Boufares, N. Chami, J.P. Torré, D. Dalmazzone, L. Fournaison, A. Delahaye, Rheological properties of CO2 hydrate slurries in presence of dioctyl sodium sulfosuccinate (AOT) in a dynamic loop for refrigeration application, Chem. Eng. Sci. 275 (2023) 118716.
[34] J. Oignet, A. Delahaye, J.-P. Torré, C. Dicharry, H.M. Hoang, P. Clain, V. Osswald, Z. Youssef, L. Fournaison, Rheological study of CO2 hydrate slurry in the presence of Sodium Dodecyl sulfate in a secondary refrigeration loop, Chem. Eng. Sci. 158 (2017) 294–303.
[35] J.-P. Torré, C. Dicharry, M. Ricaurte, D. Daniel-David, D. Broseta, CO2 capture by hydrate formation in quiescent conditions: in search of efficient kinetic additives, Energy Procedia 4 (2011) 621–628.
[36] T.K. De, A. Maitra, Solution behaviour of aerosol OT in non-polar solvents, Adv. Colloid Interface Sci. 59 (1995) 95–193, https://doi.org/10.1016/0001-8686(95)80005-N.
[37] T. Nishimi, C.A. Miller, Spontaneous emulsification of oil in Aerosol-OT/water/hydrocarbon systems, Langmuir (2000), https://doi.org/10.1021/la0006521.
[38] W.I. Higuchi, R. Okada, A.P. Lemberger, Aggregation in oil-in-water emulsions. Effects of dioctyl sodium sulfosuccinate concentration, J. Pharm. Sci. (1962), https://doi.org/10.1002/jps.2600510717.
[39] E. Günther, T. Schmid, H. Mehling, S. Hiebler, L. Huang, Subcooling in hexadecane emulsions, Int. J. Refrig. 33 (2010) 1605–1611, https://doi.org/10.1016/j.ijrefrig.2010.07.022.
[40] X. Zhang, J. Niu, S. Zhang, J.-Y. Wu, PCM in water emulsions: supercooling reduction effects of nano-additives, viscosity effects of surfactants and stability, Adv. Eng. Mater. 17 (2015) 181–188, https://doi.org/10.1002/adem.201300575.
[41] T. Morimoto, H. Kumano, Flow and heat transfer characteristics of phase change emulsions in a circular tube: part 1. Laminar flow, Int. J. Heat Mass Transf. (2018 a), https://doi.org/10.1016/j.ijheatmasstransfer.2017.10.055.
[42] T. Morimoto, H. Kumano, Flow and heat transfer characteristics of phase change emulsions in a circular tube: part 2. turbulent flow, Int. J. Heat Mass Transf. (2018 b), https://doi.org/10.1016/j.ijheatmasstransfer.2017.10.052.
[43] T. Morimoto, K. Togashi, H. Kumano, H. Hong, Thermophysical properties of phase change emulsions prepared by D-phase emulsification, Energy Convers. Manag. 122 (2016) 215–222, https://doi.org/10.1016/j.enconman.2016.05.065.
[44] T. Kawanami, K. Togashi, K. Fumoto, S. Hirano, P. Zhang, K. Shirai, S. Hirasawa, Thermophysical properties and thermal characteristics of phase change emulsion for thermal energy storage media, Energy 117 (2016) 562–568, https://doi.org/10.1016/j.energy.2016.04.021.
[45] J. Chen, P. Zhang, Preparation and characterization of nano-sized phase change emulsions as thermal energy storage and transport media, Appl. Energy 190 (2017) 868–879, https://doi.org/10.1016/j.apenergy.2017.01.012.
[46] X. Zhang, J. Niu, J.-Y. Wu, Development and characterization of novel and stable silicon nanoparticles-embedded PCM-in-water emulsions for thermal energy storage, Appl. Energy (2019), https://doi.org/10.1016/j.apenergy.2019.01.159.
[47] F. Giordano, S. Gschwander, Evaluation of energy density in hexadecane phase change emulsions in comparison to water, Int. J. Energy Res. 2024 (2024) 4021812, https://doi.org/10.1155/2024/4021812.
[48] M. Shayanmehr, F. Eslami, Stability of n-hexadecane phase change material emulsions using sugar-based surfactants and the HLD platform, J. Surfactants Deterg. 27 (2024) 567–579, https://doi.org/10.1002/jsde.12745.
[49] S.-M. Cui, S. Hashmi, W.-Q. Li, S. Handschuh-Wang, C.-T. Zhu, S.-C. Wang, Y.-F. Huang, G.-M. Zhu, F.J. Stadler, Rheology of graphene oxide stabilized pickering emulsions, Soft Matter (2023), https://doi.org/10.1039/d3sm00314k.
[50] L. Liu, J. Niu, J.-Y. Wu, Formulation of highly stable PCM nano-emulsions with reduced supercooling for thermal energy storage using surfactant mixtures, Sol. Energy Mater. Sol. Cells 223 (2021) 110983, https://doi.org/10.1016/j.solmat.2021.110983.
[51] S. Mo, J. Chen, Y. Yu, Yufen Chen, L. Jia, Ying Chen, Development and thermal characteristics of phase change nanoemulsions for low-temperature thermal energy storage, Int. J. Refrig. 161 (2024) 113–123, https://doi.org/10.1016/j.ijrefrig.2024.02.018.
[52] M.A. Torlopov, I.N. Vaseneva, V.I. Mikhaylov, I.S. Martakov, P.V. Legki, P. A. Sitnikov, Chitin nanocrystals/alginate complex for tuning stability, rheology and bioavailability of cholecalciferol in pickering emulsions, Int. J. Biol. Macromol. (2024), https://doi.org/10.1016/j.ijbiomac.2024.130671.
[53] V. Prakash, L. Parida, Characterization and rheological behavior of vitamin E nanoemulsions prepared by phase inversion composition technique, Results Eng 18 (2023) 101175, https://doi.org/10.1016/j.rineng.2023.101175.
[54] F. Salehi, K. Samary, M. Tashakori, Influence of organic acids on the viscosity and rheological behavior of guar gum solution, Results Eng 22 (2024) 102307, https://doi.org/10.1016/j.rineng.2024.102307.
[55] E.B. Webb, C.A. Koh, M.W. Liberatore, Rheological properties of methane hydrate slurries formed from AOT+ water+ oil microemulsions, Langmuir 29 (2013) 10997–11004.
[56] J.J. Buzolic, H. Li, Z.M. Aman, D.S. Silvester, R. Atkin, Surface-active ionic liquids as lubricant additives to hexadecane and diethyl succinate, Colloids Surf. Physicochem. Eng. Asp. 699 (2024) 134669, https://doi.org/10.1016/j.colsurfa.2024.134669.
[57] P. Clain, A. Delahaye, L. Fournaison, N. Mayoufi, D. Dalmazzone, W. Fürst, Rheological properties of tetra-n-butylphosphonium bromide hydrate slurry flow, Chem. Eng. J. 193 (2012) 112–122.
[58] A. Delahaye, L. Fournaison, S. Marinhas, M.C. Martínez, Rheological study of CO2 hydrate slurry in a dynamic loop applied to secondary refrigeration, Chem. Eng. Sci. 63 (2008) 3551–3559, https://doi.org/10.1016/j.ces.2008.04.001.
[59] J.F. Steffe, Rheological Methods in Food Process Engineering, Freeman press, 1996.

[60] V. Andersson, J.S. Gudmundsson, Flow properties of hydrate-in-water slurries, Ann. N. Y. Acad. Sci. 912 (2000) 322–329.
[61] L. Huang, M. Petermann, An experimental study on rheological behaviors of paraffin/water phase change emulsion, Int. J. Heat Mass Transf. 83 (2015) 479–486, https://doi.org/10.1016/j.ijheatmasstransfer.2014.12.037.
[62] H. McPhee, V. Soni, S. Saber, M. Zargartalebi, J. Riordon, M. Holmes, M. Toews, D. Sinton, Rheological behavior of phase change slurries for thermal energy applications, Langmuir (2023), https://doi.org/10.1021/acs.langmuir.2c02279.
[63] T.D. Jakobsen, S. Simon, E.B. Heggset, K. Syverud, K. Paso, Interactions between surfactants and cellulose nanofibrils for enhanced oil recovery, Ind. Eng. Chem. Res. 57 (2018) 15749–15758, https://doi.org/10.1021/acs.iecr.8b04206.
[64] S. Haouache, P. Clain, I. Capron, A. Delahaye, L. Fournaison, The influence of droplet size and hexadecane volume fraction on the rheological behavior of hexadecane-in-water emulsion stabilized by cellulose nanocrystals, in: 13th IIR Conference on Phase-Change Materials and Slurries for Refrigeration and Air Conditioning, Vicenza, Italy, 2021.
[65] S.-M. Cui, S. Hashmi, W.-Q. Li, S. Handschuh-Wang, C.-T. Zhu, S.-C. Wang, P.-P. Yang, Y.-F. Huang, G.-M. Zhu, F.J. Stadler, Influence of cellulose nanofibers on the behavior of pickering emulsions. Part 1, Microsc. Startup Flow Test. Mater. (2022), https://doi.org/10.3390/ma15238285.
[66] S.O. Ilyina, A.V. Vlasova, I.Y. Gorbunova, N.I. Lukashov, M.L. Kerber, S.O. Ilyin, Epoxy phase-change materials based on paraffin wax stabilized by Asphaltenes, Polymers (2023), https://doi.org/10.3390/polym15153243.
[67] L. Klochko, J. Noel, N.R. Sgreva, S. Leclerc, C. Métivier, D. Lacroix, M. Isaiev, Thermophysical properties of n-hexadecane: combined molecular dynamics and experimental investigations, Int. Commun. Heat Mass Transf. 137 (2022), https://doi.org/10.1016/j.icheatmasstransfer.2022.106234.
[68] N.R. Sgreva, J. Noel, C. Métivier, P. Marchal, H. Chaynes, M. Isaiev, Y. Jannot, Thermo-physical characterization of hexadecane during the solid/liquid phase change, Thermochim. Acta 710 (2022), https://doi.org/10.1016/j.tca.2022.179180.